Talanta 83 (2011) 1623–1633

Contents lists available at ScienceDirect

Talanta

journal homepage: www.elsevier.com/locate/talanta

Optimization of a pharmaceutical freeze-dried product and its process using an experimental design approach and innovative process analyzers

T.R.M. De Beer[a,*], M. Wiggenhorn[b], A. Hawe[c], J.C. Kasper[b], A. Almeida[d], T. Quinten[d], W. Friess[b], G. Winter[b], C. Vervaet[d], J.P. Remon[d]

[a] Laboratory of Pharmaceutical Process Analytical Technology, Department of Pharmaceutical Analysis, Ghent University, Harelbekestraat 72, B-9000 Gent, Belgium
[b] Department of Pharmacy, Pharmaceutical Technology and Biopharmaceutics, Ludwig-Maximilians-University, Butenandtstr. 5, D-81377 Munich, Germany
[c] Division of Drug Delivery Technology, Leiden/Amsterdam Center for Drug Research, Leiden University, P.O. Box 9502, 2300 RA Leiden, The Netherlands
[d] Laboratory of Pharmaceutical Technology, Department of Pharmaceutics, Ghent University, Harelbekestraat 72, B-9000 Gent, Belgium

ARTICLE INFO

Article history:
Received 15 July 2010
Received in revised form 1 November 2010
Accepted 22 November 2010
Available online 30 November 2010

Keywords:
Freeze-drying
Optimisation
Spectroscopy
Design space

ABSTRACT

The aim of the present study was to examine the possibilities/advantages of using recently introduced in-line spectroscopic process analyzers (Raman, NIR and plasma emission spectroscopy), within well-designed experiments, for the optimization of a pharmaceutical formulation and its freeze-drying process. The formulation under investigation was a mannitol (crystalline bulking agent)–sucrose (lyo- and cryoprotector) excipient system. The effects of two formulation variables (mannitol/sucrose ratio and amount of NaCl) and three process variables (freezing rate, annealing temperature and secondary drying temperature) upon several critical process and product responses (onset and duration of ice crystallization, onset and duration of mannitol crystallization, duration of primary drying, residual moisture content and amount of mannitol hemi-hydrate in end product) were examined using a design of experiments (DOE) methodology. A 2-level fractional factorial design (2^{5-1} = 16 experiments + 3 center points = 19 experiments) was employed. All experiments were monitored in-line using Raman, NIR and plasma emission spectroscopy, which supply continuous process and product information during freeze-drying. Off-line X-ray powder diffraction analysis and Karl-Fisher titration were performed to determine the morphology and residual moisture content of the end product, respectively.

In first instance, the results showed that – besides the previous described findings in De Beer et al., Anal. Chem. 81 (2009) 7639–7649 – Raman and NIR spectroscopy are able to monitor the product behavior throughout the complete annealing step during freeze-drying. The DOE approach allowed predicting the optimum combination of process and formulation parameters leading to the desired responses. Applying a mannitol/sucrose ratio of 4, without adding NaCl and processing the formulation without an annealing step, using a freezing rate of 0.9 °C/min and a secondary drying temperature of 40 °C resulted in efficient freeze-drying supplying end products with a residual moisture content below 2% and a mannitol hemi-hydrate content below 20%. Finally, using Monte Carlo simulations it became possible to determine how varying the factor settings around their optimum still leads to fulfilled response criteria, herewith having an idea about the probability to exceed the acceptable response limits. This multi-dimensional combination and interaction of input variables (factor ranges) leading to acceptable response criteria with an acceptable probability reflects the process design space.

1. Introduction

The overall aim of the present paper is to examine whether some recently presented spectroscopic in-line freeze-drying process analyzers (Process Analytical Technology tools) applied in well-designed experiments utilizing design of experiments can advantageously supplement the traditional freeze-drying process development and optimization of a pharmaceutical formulation.

Process Analytical Technology (PAT) is a concept, proposed by the US Food and Drug Administration (FDA) in 2004, which is expected to lie at the basis of the pharmaceutical "Good Manufacturing Practice" rules for the 21st century [1]. By means of scientific, risk-based PAT frameworks, it is aimed to design and develop continuously monitored and controlled, well understood and efficient processes that will consistently ensure a predefined quality at the end of the manufacturing process. This will be done by timely in-

* Corresponding author. Tel.: +32 9 2648097; fax: +32 9 2648196.
E-mail address: Thomas.DeBeer@UGent.be (T.R.M. De Beer).

0039-9140/$ – see front matter © 2010 Elsevier B.V. All rights reserved.
doi:10.1016/j.talanta.2010.11.051

line, on-line or at-line measurements of the critical intermediate steps and endpoints during the process. To fulfill the PAT objectives in a process, it is necessary to apply a suitable combination of PAT tools, amongst others process analyzers, multivariate data-analysis tools, endpoint monitoring tools and knowledge management tools [1]. PAT fits well into the paradigm shift in pharmaceutical manufacturing from a quality-by-design (QbD) perspective, as discussed in the regulatory guidelines ICH Q8, Q9 and Q10.

Hawe and Friess recently investigated the suitability of combining the crystalline bulking agent mannitol with the lyo- and cryoprotector sucrose as alternative excipient system to the combination human serum albumin (HSA) – mannitol for the stabilization of a hydrophobic cytokine formulation during freeze-drying [2,3]. The reasons for replacing HSA as a lyoprotector and cryoprotector during lyophilization are profoundly explained in [3]. As HSA is gained from human plasma, its use is always related to the risk of blood-born pathogens, as well as batch-to-batch variations. Furthermore, specific analytics for the active protein (cytokine) are difficult in the presence of an excess of HSA. The alternative mannitol–sucrose formulation development and its freeze-drying cycle optimization were adequately performed using traditionally applied techniques and experiments. Differential scanning calorimetry (DSC) and Low-temperature X-ray Powder Diffraction (LTXRD) were used to study the frozen solutions, while after lyophilization the products were analyzed with DSC, Temperature-modulated DSC (TMDSC), X-ray Powder Diffraction (XRD) and Karl-Fisher titration.

The aim of this study was to examine whether some recently introduced in-line spectroscopic process analyzers (Raman and NIR spectroscopy and plasma emission spectroscopy) [4], supplying continuous process (e.g., intermediate process step endpoints) and product information during freeze-drying, can advantageously contribute to the optimization of this alternative mannitol–sucrose formulation and its freeze-drying process, and confirm the earlier obtained findings and conclusions. Continuously collected in-line product information might lead to increased understanding of the formulation behavior during processing, hence allowing to increase product quality and process efficiency. Herewith, a design of experiments (DOE) methodology was applied. Studying the effects of several formulation and process parameters upon critical process parameters and (intermediate) product quality attributes by trial-and-error or by changing one separate factor at a time (COST) strategies are inefficient as the data from these experiments do not enable to identify interaction effects between the variables [5]. Moreover, the COST approach often does not lead to the optimum solution within the investigated space, while DOE analysis supplies an overview of how all studied responses (i.e., critical process and formulation aspects) behave within the investigated space from the examined process and formulation settings. Finally, DOE allows determining a design space around the optimum settings within which the desired responses are guaranteed.

Raman, NIR and plasma emission spectroscopy (Lyotrack) were recently proposed as innovative and complementary in-line monitoring tools for freeze-drying processes [4]. These PAT tools do not only complement each other but may also confirm and correct each other. The monitoring set up of the Raman and NIR process analyzers shown in this previous study cannot be applied (yet) at industrial scale, mainly because only one vial is monitored. However, multiplex systems coupling several probes to the spectrometer might serve a solution by monitoring these vials covering the largest variation in the freeze-drier. The major technical challenge remains at interfacing these sensors in an industrial freeze-drying GMP environment. Raman and NIR spectroscopy are the first tools allowing to look directly into the product during freeze-drying, and might hence supply a valuable contribution to the process and product optimization. Lyotrack measures the humidity in the drying chamber and has demonstrated good sensitivity and reproducibility to determine the primary and secondary drying endpoints. Since Lyotrack involves ionization of the gas present in the chamber, there is a potential risk to stability of the product via free radical oxidation [6]. Critical evaluation of this tool can be found in [6,7].

To the best of our knowledge, the combination of these PAT tools has not been used yet for the in-line monitoring of a pharmaceutical freeze-drying process and for the process and formulation optimization using a DOE approach.

2. Materials and methods

2.1. Materials

Mannitol was obtained from VWR International (Fontenay sous Bois, France), sucrose from Suedzucker (Mannheim, Germany), polysorbate 20 from Serva (Heidelberg, Germany) and glycine and NaCl from Sigma (Steinheim, Germany).

2.2. Experimental setup and process description

All freeze-drying experiments were performed in an Epsilon 2–6 D freeze-dyer (Christ, Osterrode, Germany). For the in-line and real-time spectroscopic monitoring, the plasma ionization device probe was mounted directly on top of the freeze-dyer chamber (Fig. 1a and b). Raman and NIR non-contact probes were built into the freeze-dyer chamber (Fig. 1a and b). Non-contact probes are required as contact of measurement tools with the freeze-dried product potentially influences process and product, making the monitored vials unrepresentative for the other vials. The fiber optic cables connecting the Raman and NIR probes to the respective spectrometers, were guided through the port in the sidewall of the freeze-dryer chamber. The Raman probe, positioned on top of a vial, and the NIR probe, placed in front of the sidewall at the bottom of a vial (i.e., NIR measurements done through the glass vial in contrast to the Raman measurements), were each focused on a different vial for reasons described in our previous study [8]. Focusing both probes on the same vial results in saturated Raman spectra, as the non-absorbed NIR light is reflected to the Raman probe, hence being collected together with the Raman scattering. The position of the Raman probe (top) and NIR probe (side wall) to the monitored vials is also discussed in [8].

2.3. Measurement tools

2.3.1. Raman spectroscopy

A RamanRxn1 spectrometer (Kaiser Optical Systems, Ann Arbor, MI, USA), equipped with an air-cooled charge coupled device (CCD) detector (back-illuminated deep depletion design) was used in combination with a fiber-optic non-contact probe to monitor the lyophilization processes in-line and non-invasive. As the Raman probe was directly focused on the product to be freeze-dried, the glass vial did not interfere with the Raman signal. The laser wavelength during the experiments was the 785 nm line from a 785 nm Invictus NIR diode laser. All spectra were recorded at a resolution of 4 cm^{-1} using a laser power of 400 mW. Data collection, data transfer, and data analysis were automated using the HoloGRAMS™ data collection software (Kaiser Optical Systems), the HoloREACT™ reaction analysis and profiling software (Kaiser Optical Systems), the Matlab software (The Mathworks; version 7.7), and the Grams/AI-PLSplusIQ software (Thermo Scientific; version 7.02). Thirty-two exposures were used for in-line monitoring of freeze-drying. Spectra were collected every 2 min

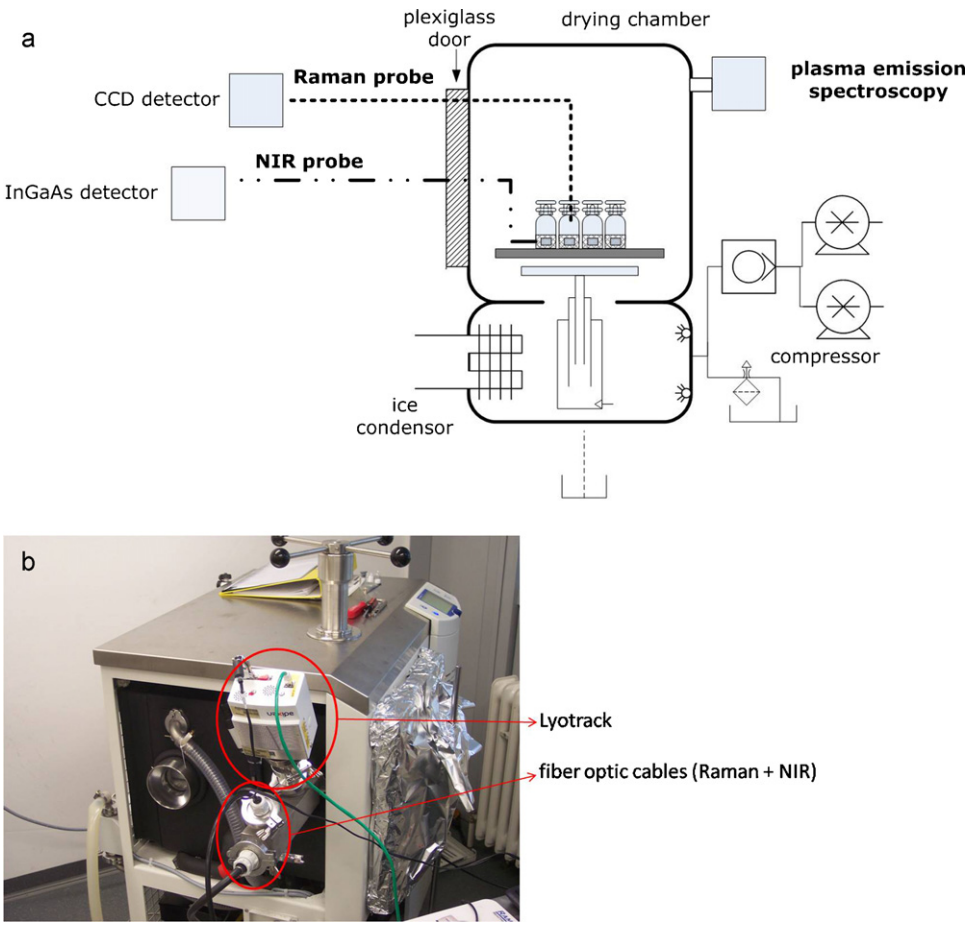

Fig. 1. (a) Schematic in-line monitoring experimental setup. (b) Experimental setup: the fiber optic cables connecting the Raman and NIR probes to the respective spectrometer, were guided through the port in the sidewall of the freeze dyer chamber.

and preprocessed by baseline correction (Pearson's method) before data-analysis.

2.3.2. NIR spectroscopy

Diffuse reflectance NIR spectra were continuously collected in-line and non-invasive during freeze-drying using a Fourier-Transform NIR spectrometer (Thermo Fisher Scientific, Nicolet Antaris II near-IR analyzer) equipped with an InGaAS detector, a quartz halogen lamp and a fiber optic non-contact probe, which was placed next to the vial. Data analysis was done using Thermo Fisher Scientific's Result software, SIMCA-P (Umetrics, version 11) and Matlab (The Mathworks, version 7.7). Each spectrum was collected in the 10,000–4000 cm^{-1} region with a resolution of 16 cm^{-1} and averaged over 32 scans. All spectra were preprocessed using standard normal variate transformation (SNV) and mean centered before data-analysis.

2.3.3. Plasma emission spectroscopy

The applied cold plasma ionization device (Lyotrack 100, Adixen, France) is based on the Inductive Coupled Plasma/Optical Emission Spectroscopy (ICP/OES) technique, allowing in-line and real-time water vapor determination in the freeze-dyer chamber during drying [7]. The device is composed of a quartz tube which directly contacts the lyophilization chamber, and is connected directly to the freeze-dryer ports on top of the freeze-dryer chamber. As water vapor is led to the condenser, the Lyotrack system is supposed to be able to detect the primary and secondary drying endpoints.

Two gasses are mainly present in a freeze-dyer during drying: water vapor originating from the formulation to be dried and nitrogen from the pressure regulation. The pressure during drying in the freeze-dyer is air-regulated, air consisting of about 80% nitrogen. The radiofrequency source (440 MHz) from the plasma ionization device creates a cold plasma in the quartz tube under vacuum (i.e., <3 mbar). The electrons from the gas atoms and molecules in the freeze-dryer are moved to a discrete higher energy state by absorbing this radiofrequency energy. The electrons spontaneously return to their normal state and release this energy by emitting a photon. The wavelength of these photons is characteristic for each molecule and atom. The emitted photons are collected with an optical fiber and diffracted with an optical spectrometer. The optical spectrum is analyzed by the plasma sensor software and the humidity curve, varying between 0 (no water vapor) and 1 (saturated with water vapor), is displayed in real-time as the ratio of water vapor to nitrogen (labeled as humidity in the software) during the drying steps.

2.3.4. X-ray powder diffraction (XRD)

The morphology of the lyophilized products was analyzed using an X-ray powder diffraction (XRD) from 5 to 30° 2θ, with steps of 0.05° 2θ and a duration of 2 s per step on the X-ray diffractometer XRD 3000 TT (Seifert, Ahrenburg, Germany), equipped with a copper anode (40 kV, 30 mA, wavelength 154.17 pm).

2.3.5. Karl-Fisher titration

The residual moisture content of the samples was determined by colorimetric Karl-Fisher titration using the Aqua 40.00 titrator with headspace module (Analytik Jena AG, Halle, Germany). For the measurements, at least 10 mg of the lyophilized sample was heated to 80 °C for 10 min. The evaporated water was trans-

Table 1
Equipment, formulation and process factors affecting the freeze-drying process performance and product quality attributes.

	Quality attributes	
	Residual moisture content	
	Tg	
	API and excipient solid state	
	API stability	
	Hydrate content	
	Aggregate formation	
	Presence of particles	
	Cake elegance	
	Reconstitution time	
Equipment variables	**Formulation attributes**	**Process parameters**
Freeze-dyer type and characteristics	*Initial*	*Freezing*
	API and its concentration	Freezing rate
	Excipients and their concentration	Freezing shelf temperature
	Vial type	Annealing time
	Filling volume	Annealing temperature
		Supercooling
	During processing	*Primary drying*
	Tg'	Shelf temperature
	Tcollapse	Ramp to reach shelf temp.
	Tproduct	Duration
	Teutectic	Chamber pressure
		Secondary drying
		Shelf temperature
		Ramp to reach shelf temp.
		Duration
		Chamber pressure

ferred into the titration solution and the amount of water was determined. As reference material, Apura Water Standard Oven 1% (Merck, Darmstadt, Germany) was used and the recovery was considered for the calculation of the residual moisture of the samples.

2.4. Experimental design methodology

Most process and formulation parameters, which are generally critical for a freeze-drying process and which affect the final quality attributes, are summarized in Table 1 (as proposed in [5]). In the present study, the effects of two formulation variables (mannitol/sucrose ratio and amount of NaCl) and three process variables (freezing rate, annealing temperature and secondary drying temperature) upon several process and product quality responses (Table 2) were examined. These variables were selected as the previous study from Hawe and Friess showed them to be most influencing on process performance and product quality [2]. All other parameters were kept constant (Table 2). The same type of vials (2R Schott, Mainz, Germany) was used throughout all freeze-drying experiments.

For the HSA-free formulations, a total solid content of 5.0% (w/v) was selected with mannitol as crystalline bulking agent and sucrose as amorphous lyo- and cryoprotector. The optimum ratio of both excipients upon the examined response variables (Table 2) was evaluated. Herewith, the addition of NaCl was examined as small NaCl amounts can lead to significant changes of the physicochemical properties of mannitol and sucrose during freeze-drying. NaCl is used in HSA containing formulations as NaCl has a stabilizing effect preserving HSA from (heat-induced) aggregations and particle formation. The necessity of NaCl in the HSA-free formulations was therefore examined as well. Also the need of including annealing was examined, as annealing can help to maximize crystallization of the bulking agent during freezing. Furthermore, annealing can influence the final product solid state. Further, a closer look was taken on the influence of the freezing rate (i.e., the temperature decrease in function of time) upon the response variables as the freezing rate is related to the degree of supercooling and the rate of ice crystallization. The degree of supercooling determines the number of ice crystals formed and hence the product resistance during drying. The rate of ice crystal growth determines the residence time of the product in a freeze-concentrated fluid state [9]. Finally, the requirement of performing secondary drying at high temperatures was evaluated. During freezing, mannitol has a tendency to crystallize partly into mannitol hemi-hydrate, which can lead to stability problems during storage due to hydrate water release and conversion into anhydrous crystal forms. Secondary drying at high temperatures (40 °C) might avoid the presence of the hemi-hydrate forms at the end of freeze-drying processing [10].

Table 2 shows the investigated space within which the selected DOE parameters were varied. All variables were considered as continuous variables. A 2-level fractional factorial screening design (= 2^{5-1} = 16 experiments + 3 center points = 19 experiments) was employed. This is a resolution V design, indicating that the main effects are unconfounded with two-factor interactions and that two-factor interactions are unconfounded with each other. An overview of the performed DOE experiments is given in Table 3.

2.5. Process analysis

As three process analyzers were applied to continuously collect data during the freeze-drying processes, a huge amount of complex data was obtained per process. As 1 Raman and 1 NIR spectrum were obtained every 2 min during the processes, which sometimes took over 20 h, chemometric tools were necessary to extract useful information from the large data sets. The plasma data were ana-

Table 2
Varied DOE factors with their examined design space. Column 4 shows the DOE response variables, while column 5 lists the parameters which were fixed.

Examined parameters	Levels (design space)		Response variables	Process and formulation parameters kept constant
	–	+		
Mannitol/sucrose	1	4	*Process related*	Total excipient amount: 5% (w/v)
NaCl addition (%)	0	0.2	Start ice nucleation	Filling volume: 2ml
Freezing rate (°C/min)	0.45	0.9	Duration ice nucleation	Freezing temperature: −50 °C
Annealing temperature (°C)	−50	−20	Start mannitol crystallization	Annealing time: 2 h
Sec. drying temperature (°C)	20	40	Duration mannitol crystallization	Prim. drying temp.: −15 °C
			Duration annealing	Prim. drying pressure: 0.045 mbar
			Duration primary drying	Primary drying time: 10 h
			Duration secondary drying	Sec. drying pressure: 0.045 mbar
			Intermediate solid state	Secondary drying time: 4 h
			End product related	Vial type: 2R
			End product solid state	0.005% polysorbate 20
			Mannitol hydrate content	20 mM glycine buffer pH 4.5
			Residual moisture content (%)	

Table 3
A 2-level fractional factorial design (2^{5-1} = 16 experiments + 3 center points = 19 experiments) was employed. Overview of experiments.

Experiment number	Run number	Mannitol/sucrose	NaCl (%)	Freezing rate (°C/min)	Annealing temperature (°C)	Secondary drying temperature (°C)
1	2	1	0	0.45	−50	40
2	14	4	0	0.45	−50	20
3	17	1	0.2	0.45	−50	20
4	4	4	0.2	0.45	−50	40
5	10	1	0	0.9	−50	20
6	1	4	0	0.9	−50	40
7	15	1	0.2	0.9	−50	40
8	11	4	0.2	0.9	−50	20
9	12	1	0	0.45	−20	20
10	13	4	0	0.45	−20	40
11	16	1	0.2	0.45	−20	40
12	8	4	0.2	0.45	−20	20
13	9	1	0	0.9	−20	40
14	7	4	0	0.9	−20	20
15	5	1	0.2	0.9	−20	20
16	3	4	0.2	0.9	−20	40
17	19	2.5	0.1	0.675	−35	30
18	6	2.5	0.1	0.675	−35	30
19	18	2.5	0.1	0.675	−35	30

lyzed univariately as only one data point per process time point was obtained.

The Raman and NIR spectra collected per monitored freeze-drying process were each introduced into a data matrix (**D**), resulting in an NIR data matrix and a Raman data matrix per process. Each **D** was analyzed using principal component analysis (PCA).

Analysis of the DOE results was performed using the MODDE software (Version 9.0, Umetrics, Umeå, Sweden). PCA models were developed using SIMCA-P+ software (Version 12.0.1, Umetrics, Umeå, Sweden) and Matlab 7.1 (The MathWorks, Inc., Natick, MA).

3. Results and discussion

3.1. Process analysis

Multivariate data-analysis of the in-line collected spectroscopic data will not be outlined in detail as this was thoroughly done in our previous work [4,8]. All relevant information obtained from the in-line Raman, NIR and plasma emission spectroscopic measurements during all DOE experiments is summarized in Table 4. As in-line spectroscopic monitoring of annealing has not been described yet, we will provide the Raman and NIR spectroscopic observations made during annealing of DOE experiment number 12. Annealing was evaluated as a DOE factor in this study as it might be useful for the examined formulation to maximize mannitol crystallization during freezing, as mannitol is aimed to serve as bulking agent. Since annealing is part of the freezing step of lyophilization, Raman spectroscopy is the preferable tool for annealing monitoring, as the broad ice bands overwhelm the product signals, and hence the annealing information, in the NIR spectra. Fig. 2 shows the evolution of the Raman intensity deriving from crystalline mannitol (1000–1170 cm^{-1}) during the freezing step and a major part of the primary drying step. After 186 min, the shelf temperature is increased from −50 °C to −20 °C to start annealing. Herewith, crystalline mannitol bands gradually appear in the Raman spectra. No peaks for crystalline mannitol are detected prior to the start of the annealing step, pointing at mainly amorphous mannitol being present after the initial freezing to −50 °C. After 288 min, the mannitol signals in the Raman spectra remain stable, indicating that the crystallization of mannitol during the annealing is finished. After 337 min, the shelf temperature is lowered in 30 min to −50 °C. This shelf temperature decrease and its concomitant product temperature decrease resulted in a mannitol Raman band intensity increase. Raman intensity is temperature dependent as can seen from Placzek's equation, describing the Raman intensity.

$$I = cte\left(\frac{\nu_0 + \nu_v}{\nu_v}\right)^4 \frac{NI_0}{1 - e^{(-h\nu_v/kT)}}[45(\alpha^S)^2 + 13(\alpha^a)^2] \quad (1)$$

where ν_0 is the frequency of the incident radiation, ν_v is the vibration frequency of the molecule, N is the number of irradiated Raman active molecules, I_0 is the power of the light source, h is Planck's constant (= 6.6260×10^{-34} J s), k is the Boltzman's constant, T is the temperature, α^S is the polarizability from the molecules causing Stokes radiation, and α^a is the polarizability from the molecules causing anti-Stokes radiation.

After 427 min, the shelf temperature was increased to −15 °C before introducing the vacuum, resulting in decreased mannitol band intensities (i.e., approximately the same intensity as at the end of the annealing step at −20 °C). Once vacuum was introduced (after 457 min), the Raman intensity started to increase strongly. An explanation can be further mannitol crystallization during primary drying as mannitol is known to crystallize only partly during the freezing step. Hawe and Friess described the partial crystallization during cooling of a 5% mannitol solution, with further crystallization at −19.3 °C during rewarming of the sample [2]. Moreover, the presence of sucrose in the formulation is known to inhibit mannitol crystallization during freezing [2]. Apparently, annealing is not sufficient for complete mannitol crystallization. The removal of the icy structure (primary drying) around amorphous mannitol most likely stimulates the conversion to a higher degree of crystallinity.

The NIR data analysis and interpretation was performed as in [8] and the observations are listed in Table 4. Fig. 3a shows the NIR spectral changes occurring during the annealing step of experiment 12, after ice crystallization was finished. The NIR spectra of the frozen mannitol solutions clearly change with the altered shelf temperatures involved with the annealing process. Increasing the shelf temperature from −50 °C to −20 °C results in a lower absorption in the 6471.93–5700.55 cm^{-1} region and a higher absorption in the 5314.85–4543.47 cm^{-1} region. Furthermore, the NIR spectra collected during annealing become more smoothed indicating mannitol crystallization. This is in agreement with our previous observations that the broad ice bands are less serrated when crystalline mannitol is present (the sample is less transparent) [8]. After annealing, the shelf temperature was lowered again to −50 °C, resulting in an increased absorption in the 6471.93–5700.55 cm^{-1} region and a decreased absorption in the 5314.85–4543.47 cm^{-1} region. Before vacuum introduction at the beginning of primary

Table 4
Results of DOE experiments per evaluated response variable.

Experiment number	Response 1 (Raman/NIR) Onset ice crystallization (min)	Response 2 (Raman/NIR) Duration of ice crystallization (min)	Response 3 (Raman) Start mannitol crystallization (min)	Response 4 (Raman) Duration mannitol crystallization (min)	Response 5 (plasma) Duration of primary drying (min)	Response 6 (Karl-Fisher) Residual moisture content (%)	Response 7 (Raman/XRD) Relative hemi-hydrate content (%)
1	72	44	432	116	452	2.1/1.9	17.5
2	78	30	450	146	462	2.2/2.5	35.1
3	76	36	452	106	427	3.2/3.1	28.4
4	58	46	446	116	525	2.6/2.7	7.1
5	38	44	394	528	472	2.7/2.7	35.3
6	50	50	368	160	603	2.0/2.0	16.7
7	42	10	442	44	433	2.4/2.0	21.0
8	40	32	378	100	533	2.7/2.9	30.6
9	74	32	202	408	442	2.0/1.9	38.3
10	78	34	194	314	560	2.0/1.9	24.1
11	64	28	206	362	490	3.0/2.5	28.6
12	72	12	198	376	455	2.8/2.5	58.3
13	38	14	152	340	405	2.7/2.9	45.2
14	36	20	176	284	506	2.2/2.1	51.9
15	44	16	228	462	519	3.6/3.2	42. 6
16	34	34	142	286	493	2.6/2.3	26.0
17	50	20	186	374	586	Missing/3.0	33.2
18	52	26	190	334	585	2.4/3.0	40.1
19	54	18	204	336	588	2.7/2.8	30.8

drying, the shelf temperature was raised to −15 °C resulting in similar NIR spectra as during annealing at −20 °C. These observations are even clearer in the PC 1 versus PC 2 scores plot obtained after PCA from the NIR spectra collected during annealing (Fig. 3b). This plot shows that the NIR spectra obtained during annealing (shelf temperature = −20 °C) and just before primary drying (shelf temperature = −15 °C) are similar. The NIR spectra collected prior to annealing (shelf temperature = −50 °C) without the presence of crystalline mannitol are different from the NIR spectra collected after annealing (shelf temperature also = −50 °C) where crystalline mannitol was present. PCA of the NIR spectra collected during primary drying showed that the broad ice bands had disappeared after 616 min (data not shown). However, because of the position of the NIR probe, NIR spectroscopy underestimates the primary drying endpoint [8]. Furthermore, the NIR spectra collected during primary drying show that, after disappearance of the broad ice bands, further water removal occurs as the water band at 5100–5200 cm^{-1} decreases (Fig. 3c). This water band decrease was not seen in previous studies where only crystalline material was present in the vial [8]. Hence, this diminishing water band suggests water removal from the amorphous sucrose phase, indicating that desorption started already during primary drying [11]. Desorption continued after the introduction of secondary drying (data not shown).

During lyophilization mannitol can crystallize in the α-, β- or δ-modification or as mannitol hemi-hydrate depending on the applied freezing protocol, a potential annealing step and the process conditions during primary and secondary drying [12–14]. Our previous studies showed that the Raman spectral differences between the different mannitol solid states (α, β, δ and hemi-hydrate) can be clearly distinguished in the 1000–1170 cm^{-1} spectral range. As all other components in the studied formulation produce no signal at 1000–1170 cm^{-1}, all visible bands in this spectral range originate from mannitol. The presence of other excipients like buffer components, lyoprotectants or proteins can both inhibit

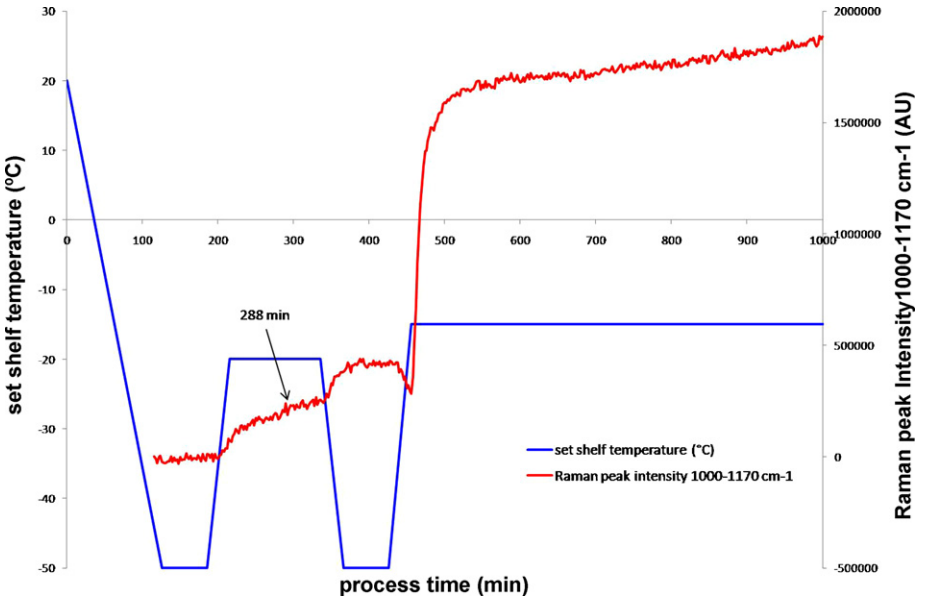

Fig. 2. Evolution of the Raman intensity of crystalline mannitol signals (1000–1170 cm^{-1}) during the freezing step and the first part of the primary drying step of experiment 12.

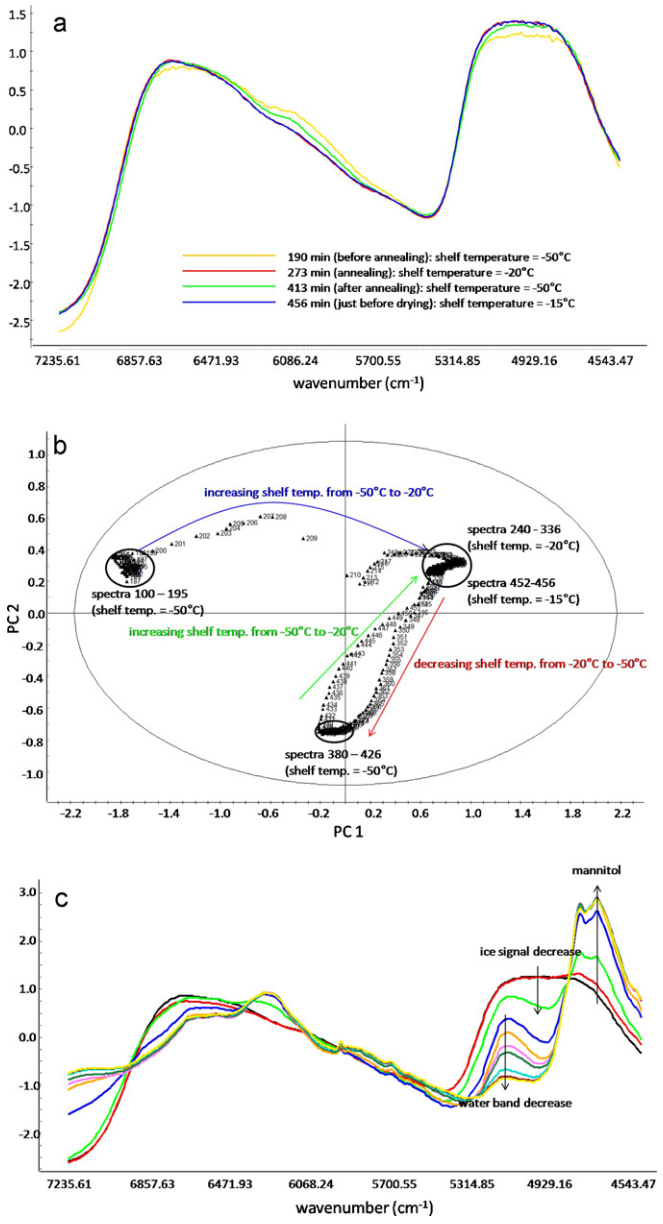

Fig. 3. (a) NIR spectral changes during the annealing step of experiment 12. (b) PC 1 versus PC 2 scores plot obtained after PCA from the NIR spectra collected during annealing of experiment 12. (c) After disappearance of the broad ice bands, further water removal occurs during primary drying as the water band at 5100–5200 cm^{-1} decreases (experiment 12).

and promote mannitol crystallization. Grohganz et al. showed that NIR spectroscopy can be used to analyze mannitol/sucrose matrix based freeze-dried samples and classify them according to composition, water content and solid-state properties [15]. The mannitol hemi-hydrate content conclusions derived from the Raman, NIR and XRD data are listed in Table 4 for all DOE experiments.

3.2. Experimental design analysis

From the experimental results (Table 4), regression models were calculated for all response variables using Modde 9.0. In first instance, the raw data were evaluated using replicate plots, in which the ideal outcome is that the variability of repeated experiments is much less than the overall variability (plots not shown). The effects of the studied variables were graphically and statistically interpreted using the Modde software and by the normal probability plot and the algorithm of Dong [16]. The significant effects and interactions are mentioned in Table 5 for each evaluated response variable. The way in which the significant factors and the significant interactions influence the response variables is shown by + (positive effect) and − (negative effect). After fitting the regression models, the goodness of fit (R^2) and the goodness of prediction (Q^2) were evaluated. The least significant regression coefficients were excluded provided that Q^2 increased.

Table 5
Significant effects and interactions per studied response variable. The way the significant factors and the significant interactions influence the response variables is shown by (+) for a positive effect and (−) for a negative effect.

Response	Significant effects and interactions
Onset ice crystallization (min)	Freezing rate (−)
Duration of ice crystallization (min)	–
Start mannitol crystallization (min)	Annealing temperature (−), freezing rate (−)
Duration of mannitol crystallization (min)	Annealing temperature (+)
Duration of primary drying (min)	–
Residual moisture content (%)	NaCl (+), secondary drying temperature (−), mannitol/sucrose (−)
Relative hemi-hydrate content (%)	Annealing (+), secondary drying temperature (−)

Table 5 shows that only the freezing rate significantly influences the onset of ice crystallization. Ice nucleation is normally a random process, varying form batch to batch and even from vial to vial within a batch [6]. However, it is evident that ice nucleation will start faster using a 0.9 °C/min freezing rate compared to a 0.45 °C/min freezing rate, as supercooling of the solution is reached earlier. No significant effect was found for the response variable duration of ice nucleation process. A previous study showed that this response is mainly affected by the volume of the freeze-dried solution [17]. This variable was not evaluated in this study.

Mannitol crystallization evidently started sooner when an annealing step was included during freezing. Furthermore, an increased freezing rate also slightly has a negative effect on the onset of mannitol crystallization, resulting in earlier mannitol crystallization. Mannitol crystallization only started after introduction of primary drying for the experiments without annealing. It is clear that for these experiments, primary drying and hence mannitol crystallization started earlier when a fast freezing rate (i.e., shorter freezing step) was applied. The duration of the complete mannitol crystallization process was evidently mainly affected by the presence of an annealing step. Even when annealing was done, mannitol crystallized only partly during freezing, and crystallized further during primary drying. Therefore, the duration of crystallization was much longer for the annealing experiments compared to the experiments without annealing and hence where mannitol crystallization only started after introducing the vacuum. A separate DOE analysis was performed for the experiments containing an annealing step and in which hence only the mannitol/sucrose ratio, the freezing rate, NaCl presence and the secondary drying temperature were varied (i.e., $2^{4-1} = 8$ experiments + 3 center points = 11 experiments). The duration of mannitol crystallization was not significantly affected by these varied variables.

The duration of primary drying is not significantly affected by any of the studied variables. The primary drying endpoints were detected using plasma emission spectroscopy as shown in [4]. In a previous study, it was demonstrated that primary drying duration is mainly affected by the initial volume of the solution in the vial [17]. In the present study, the volume was constant and low in all experiments (2 ml). Hence, the most important remaining factor influencing the primary drying time is the degree of supercooling. A high degree of supercooling results in smaller ice crystals

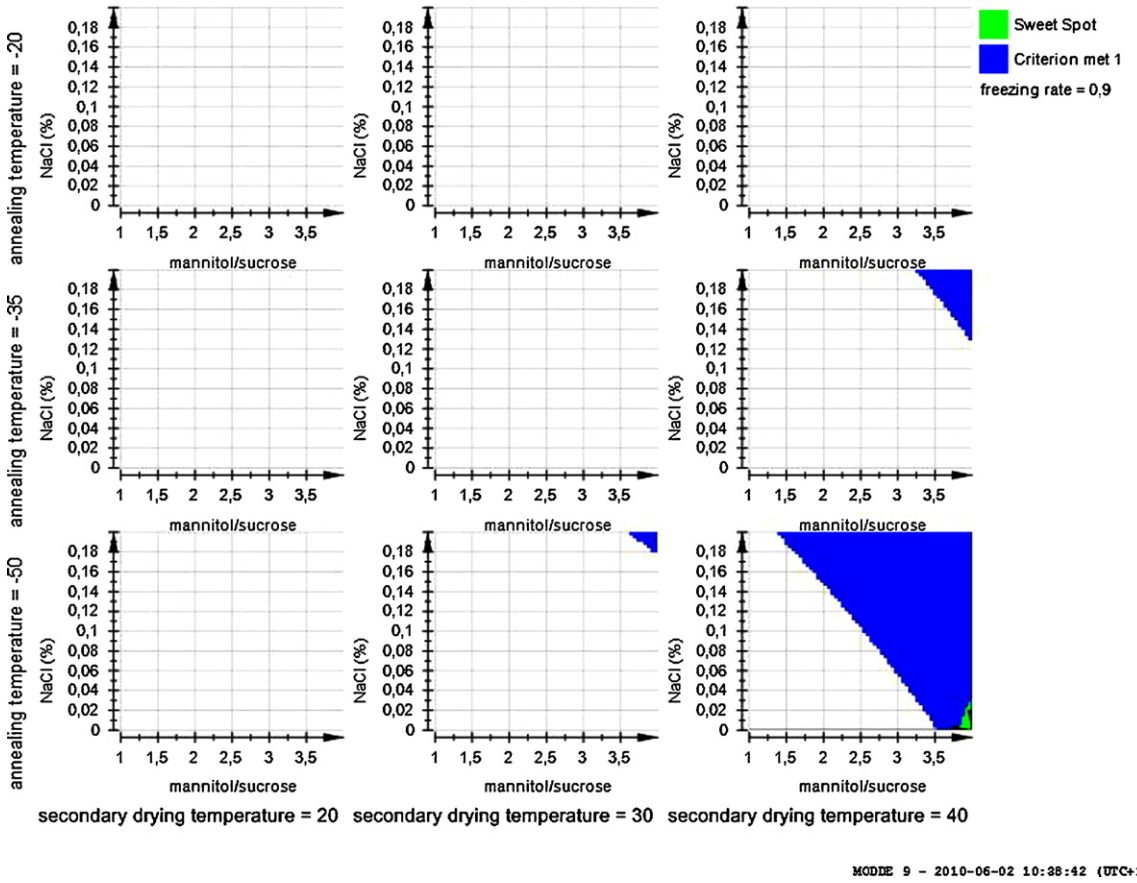

Fig. 4. The sweet spot plot highlights the combination of factors (green areas) resulting in responses within the user specified ranges (i.e., residual moisture content <2% and a mannitol hemi-hydrate content <20%). A blue area represents the combination of factors resulting in only 1 response within the aimed ranges. A white area means that none of the responses are within the desired ranges. The aimed response criteria are only met when a mannitol/sucrose ratio of 4, no NaCl, no annealing and a secondary drying temperature of 40 °C are applied. (For interpretation of the references to color in this figure legend, the reader is referred to the web version of the article.)

and hence in larger product resistance. However, ice nucleation is a random process resulting in random supercooling for the 19 DOE experiments.

Adding NaCl increased the residual moisture content, while a high secondary drying temperature and an increased mannitol/sucrose ratio decreased the residual moisture content. The residual moisture content was analyzed in duplicate per DOE experiment using Karl-Fisher titration. NaCl increases the residual moisture content within the dried product as it acts as a plasticizer of the amorphous phase [2]. A higher secondary drying temperature might facilitate the removal of water from the amorphous phases as more energy is supplied from the shelves to the vials for desorption. Furthermore, mannitol is known to crystallize (partly) into mannitol hemi-hydrate during freezing and primary drying. Previous studies showed that secondary drying stimulated the transformation from mannitol hemi-hydrate to anhydrous mannitol [17,10]. The removal of this hydrate water also contributes to apparently lower residual moisture contents when applying higher secondary drying temperatures. Increasing the mannitol/sucrose ratio resulted in lower residual moisture contents as less amorphous (hygroscopic) sucrose is present in the freeze-dried products. The secondary drying time (4 h) and applied pressure during secondary drying (45 μbar) might have been too short and too high to remove all dissolved water. Hence, more amorphous material resulted in higher residual moisture content. Usually, a pressure of 10 μbar is advised during secondary drying [2], but this was not possible in this study due to the attachment of the high number of different process analyzers to the freeze-dryer, creating some minor leaks.

The fraction of mannitol hemi-hydrate in the 19 DOE experiment end products was determined by XRD analysis as described in [2]. The relative intensity of the mannitol hemi-hydrate peak at 17.9° 2θ was considered (figure not shown, see [2]). For this relative intensity, the height of the mannitol hemi-hydrate peak was compared to the highest peak of the diffraction pattern, which was set at 100%. In an identical way, the hemi-hydrate fraction was also derived from the Raman spectra of the end products as mannitol hemi-hydrate has a band at 1150 cm^{-1} which does not appear in the Raman spectra of the anhydrous forms [17]. The average results of the Raman and XRD findings are listed in Table 4. More hemi-hydrate was observed after freeze-drying when annealing was applied. Hawe and Friess also described that annealing favored the formation of mannitol hemi-hydrate [2]. Secondary drying at 40 °C reduced the amount of hemi-hydrate as explained above. However, secondary drying at 40 °C was not able to remove all hydrated mannitol, which was also seen in [2].

3.3. Process optimization

To optimize the mannitol/sucrose formulation and its freeze-drying process, the desired response values and response limits were clearly defined. For the product quality responses, minimal residual moisture and mannitol hemi-hydrate levels were desired. With regard to process efficiency, one has to aim at the shortest freeze-drying process possible. However, all duration responses only showed small variations within the examined experimental space as can be seen from Table 4. Furthermore,

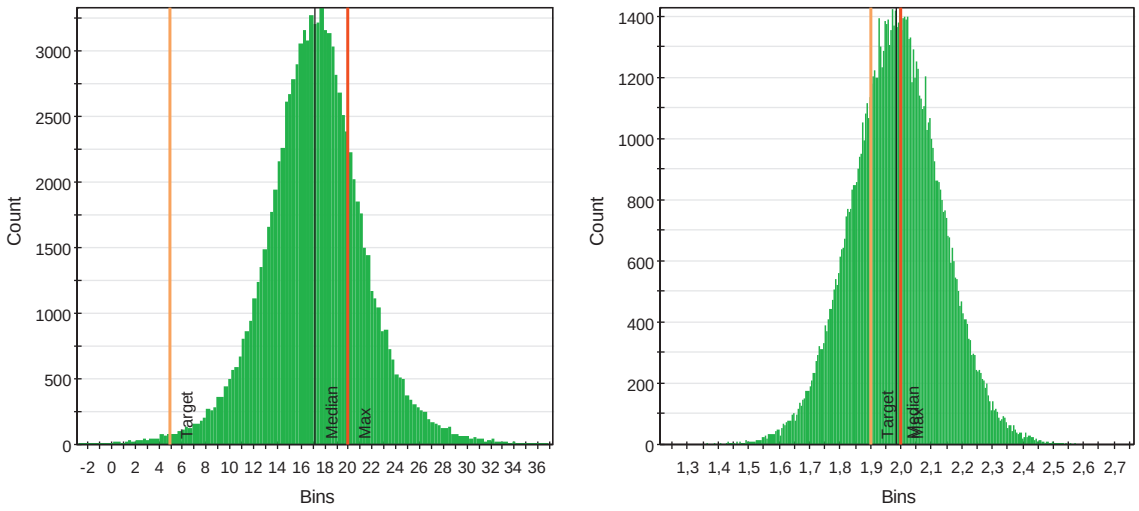

Fig. 5. Predicted response profiles for the response variables 'residual moisture content' (right) and 'amount of hemi-hydrate' (left). The yellow line represents the target value for the responses which were randomly chosen here. The red lines are the specification limits for each response (2% for residual moisture content and 20% for amount of mannitol hemi-hydrate). The green region represents the probability of a prediction when the optimum process settings are used. (For interpretation of the references to color in this figure legend, the reader is referred to the web version of the article.)

the most time consuming process step, primary drying, was not significantly influenced by any of the studied factors. Therefore, product quality optimization was prioritized over process efficiency and an optimum for the responses 'residual moisture content' and 'amount of hemi-hydrate' was searched in first instance.

The freezing rate significantly influences the onset of ice crystallization and mannitol crystallization (Table 5). Increasing the freezing rate induces a faster onset of ice and mannitol crystallization. Therefore, a freezing rate of 0.9 °C/min was selected as optimum. Using the Modde optimizer, it was possible to calculate the combination of variables resulting in our aimed responses. A residual moisture content of maximum 2.0% and a mannitol hemi-hydrate content of maximum 20% were aimed. The sweet spot plots (Fig. 4) show the regions for all combinations of examined variables where these targets are reached. The aimed response cri-

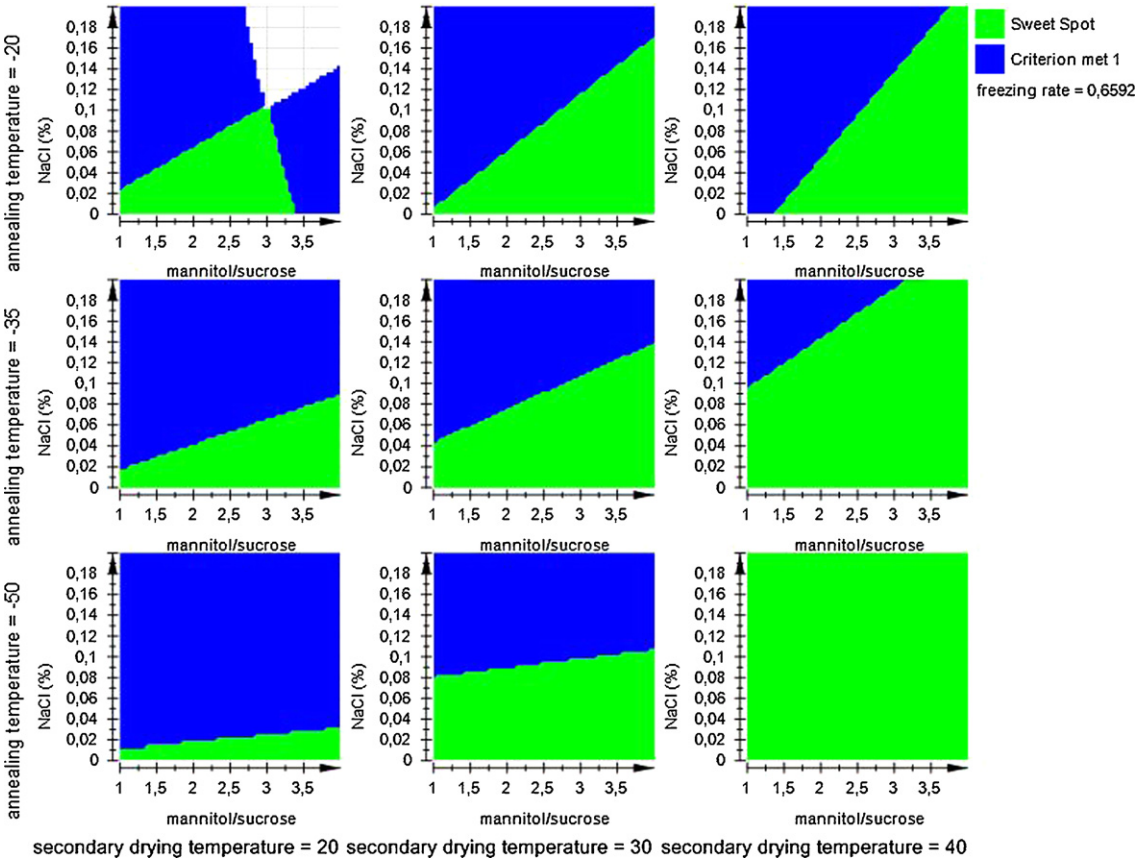

Fig. 6. Sweet spot plot highlighting the areas (green) for all combinations of examined variables where the responses are within the limits (residual moisture content <2.5% and mannitol hemi-hydrate amount <50%). (For interpretation of the references to color in this figure legend, the reader is referred to the web version of the article.)

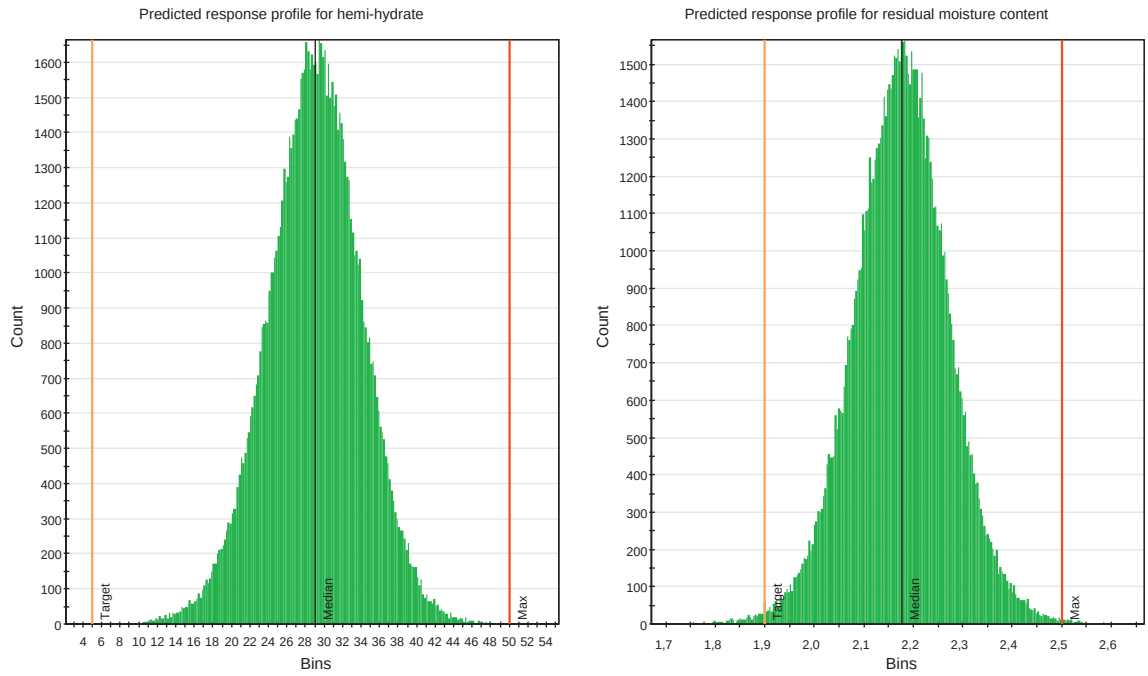

Fig. 7. Predicted response profiles for the response variables 'residual moisture content' (right) and 'amount of hemi-hydrate' (left). The yellow line represents the target value for the responses which were randomly chosen here. The red lines are the specification limits for each response (2.5% for residual moisture content and 50% for amount of mannitol hemi-hydrate). The green region represents the probability of a prediction for a random distribution of factor settings in the design space: mannitol/sucrose [2.89; 4.00], NaCl [0.000–0.012%]; freezing rate [0.50–0.82 °C/min]; annealing temperature [−45 to −20 °C]; secondary drying temperature [29.5–40.0 °C]. (For interpretation of the references to color in this figure legend, the reader is referred to the web version of the article.)

teria are only met when a mannitol/sucrose ratio of 4, no NaCl, no annealing and a secondary drying temperature of 40 °C are applied. Strict control of these optimum settings is clearly needed (which is possible for these settings) to result in minimal hemi-hydrate and moisture contents. Small disturbances in the process settings will immediately lead to undesired residual moisture and/or mannitol hemi-hydrate contents. It is clear that the obtained design space is very small and not robust. The optimum process was run two times and led to 1.9% residual moisture content and to 23% and 45% mannitol hemi-hydrate content.

Limitations with a sweet spot plot presentation are the number of dimensions and the lack of probability estimate in the predicted surface [18]. Performing Monte Carlo simulations on the found optimum factor settings showed that there is a probability of 23% for the amount of hemi-hydrate and 46% for the residual moisture content to exceed the specification limit values when the optimum process settings are used (Fig. 5).

Making the aimed responses less strict to maximum 2.5% residual moisture content and 50% mannitol hemi-hydrate enlarges the design space significantly. The sweet spot plot highlights the areas (green) for all combinations of examined variables where the responses are within these new limits (Fig. 6). The DOE models allowed to predict that combining a mannitol/sucrose of 3.44, no NaCl, a freezing rate of 0.66 °C/min, an annealing temperature of −32.60 °C and a secondary drying temperature of 34.75 °C leads to optimum responses: residual moisture content 2.2% and mannitol hemi-hydrate amount 28.97%. Based on Monte Carlo simulations on these factor settings, it became possible to determine how varying the factor settings (i.e., design space) still leads to fulfilled response criteria: mannitol/sucrose [2.89; 4.00], NaCl [0.000–0.012%]; freezing rate [0.50–0.82 °C/min]; annealing temperature [−45 to −20 °C]; secondary drying temperature [29.5–40.0 °C]. Fig. 7 shows that there is a probability of 0.00016% for the amount of hemi-hydrate and 0.0015% for the residual moisture content to exceed the specification limit values when factor settings in these ranges are used.

4. Conclusions

Within the study, the added value of applying a PAT approach, by using process analyzers, which are innovative for freeze-drying, in well-designed experiments, to the traditional COST approach, based on classical off-line quality attributes determination techniques, for the optimization of a pharmaceutical freeze-drying process was tested. The main conclusions are:

- The spectroscopic process analyzers (Raman and NIR) allowed continuous observation of the freeze-dried products during all DOE experiments. These process analyzers are the first tools allowing the continuous collection of product and process information (e.g., annealing, product solid state, water and ice behavior, residual moisture content, etc.) during the optimization of freeze-drying processes. However, it should be emphasized that these process analyzers are single vial techniques and that their current monitoring set up is still not applicable in production scale. However, the limitations for this are mainly technical issues. Multi-point spectroscopic process analyzers monitoring the vials which are covering the largest variation in a freeze-dryer might be a first important step forward.
- A DOE approach allows to determine the optimum combination of examined process and formulation parameters leading to the desired responses (i.e., critical process and formulation aspects) using a low number of experiments (19 in this study). For this freeze-drying study, the same optimum conditions were obtained as by the traditional COST approach in [2]: a mannitol/sucrose ratio of 4, no NaCl, no annealing and a secondary drying temperature of 40 °C.
- Using DOE, it becomes possible to make predictions within the investigated space. The DOE models allow predicting the studied responses when altering the studied factors. Furthermore, using Monte Carlo simulations it becomes possible to determine how varying the factor settings around the optimum factor values still leads to fulfilled response criteria, herewith having an

idea about the probability to exceed the acceptable response limits. This multi-dimensional combination and interaction of input variables (factor ranges) leading to acceptable response criteria with an acceptable probability is called the process design space.

- The DOE approach allows increasing the process understanding in terms of cause-and-effect relationships. Furthermore, significant factor interactions might become clear (however, not the case in this study). Mechanistic process modelling relies on a more fundamental understanding of the underlying physics and chemistry governing the behavior of processes, but is most difficult for complex processes.
- The process analyzers used in this study, as well as the examined factors and responses are not supplying all critical information needed for the development of a freeze-drying process. Traditional experiments such as DSC determining Tg', Tcollapse and Tg (as performed in [2]) are certainly the first needed experiments for the development and optimization of freeze-dried formulations and their processes.

References

[1] Guidance for Industry: PAT – a Framework for Innovative Pharmaceutical Development, Manufacturing, and Quality Assurance, U.S. Food and Drug Administration, September 2004 (http://www.fda.gov/downloads/Drugs/GuidanceComplianceRegulatoryInformation/Guidances/UCM070305.pdf).
[2] A. Hawe, W. Friess, Eur. J. Pharm. Biopharm. 64 (2006) 316–325.
[3] A. Hawe, W. Friess, Eur. J. Pharm. Biopharm. 68 (2008) 169–182.
[4] T.R.M. De Beer, M. Wiggenhorn, R. Veillon, C. Debacq, Y. Mayeresse, B. Moreau, A. Burggraeve, T. Quinten, W. Friess, G. Winter, C. Vervaet, J.P. Remon, W.R.G. Baeyens, Anal. Chem. 81 (2009) 7639–7649.
[5] K. Naelapää, P. Veski, H.G. Kristensen, J. Rantanen, P. Bertelsen, Pharm. Dev. Technol. 15 (2010) 35–45.
[6] S.M. Patel, M. Pikal, Pharm. Dev. Technol. 14 (2009) 567–587.
[7] Y. Mayeresse, P.H. Sibille, C. Nomine, PDA J. Pharm. Sci. Technol. 61 (2007) 160–174.
[8] T.R.M. De Beer, P. Vercruysse, A. Burggraeve, T. Quinten, J. Ouyang, X. Zhang, C. Vervaet, J.P. Remon, W.R.G. Baeyens, J. Pharm. Sci. 98 (2009) 3430–3446.
[9] M.J. Pikal, in: J. Swarbrick (Ed.), Encyclopedia of Pharmaceutical Technology, Marcel Dekker, New York, 2002, pp. 1807–1833.
[10] R. Johnson, C. Kirchhoff, H. Gaud, J. Pharm. Sci. 91 (2002) 914–922.
[11] M. Brülls, S. Folestad, A. Sparen, A. Rasmuson, Pharm. Res. 20 (2003) 494–499.
[12] A. Cannon, E. Trappler, PDA J. Pharm. Sci. Technol. 54 (2000) 13–22.
[13] A. Pyne, R. Surana, R. Suryanararyanan, Pharm. Res. 19 (2002) 901–908.
[14] X. Liao, R. Krishnamurthy, R. Suryanarayanan, Pharm. Res. 22 (2005) 1978–1985.
[15] H. Grohganz, M. Fonteyne, E. Skibsted, T. Falck, B. Palmqvist, J. Rantanen, Eur. J. Pharm. Biopharm. 74 (2010) 406–412.
[16] Y. Vander Heyden, A. Nijhuis, J. Smeyers-Verbeke, B.G.M. Vandeginste, D.L. Massart, J. Pharm. Biomed. Anal. 24 (2001) 723–753.
[17] T. De Beer, M. Allesø, F. Goethals, A. Coppens, Y. Vander Heyden, H. Lopez De Diego, J. Rantanen, F. Verpoort, C. Vervaet, J.P. Remon, W.R.G. Baeyens, Anal. Chem. 79 (2007) 7992–8003.
[18] L. Eriksson, E. Johansson, N. Kettaneh-Wold, C. Wikström, S. Wold, Design of Experiments: Principles and Applications, Umetrics Academy, 2008.